CD8+ T cells stimulated by exosomes derived from RenCa cells mediate specific immune responses through the FasL/Fas signaling pathway and, combined with GM-CSF and IL-12, enhance the anti-renal cortical adenocarcinoma effect

HAO-YU XU, NAN LI, NAN YAO, XIAO-FENG XU, HE-XI WANG, XUE-YANG LIU and YAO ZHANG

Department of Urology, The First Affiliated Hospital, Chongqing Medical University, Chongqing 400016, P.R. China

Received September 20, 2018; Accepted June 13, 2019

DOI: 10.3892/or.2019.7208

Abstract. A satisfactory cure rate for renal cell carcinoma (RCC) is difficult to achieve through traditional immunotherapy. RCC has a relatively high spontaneous regression rate due to tumor immune escape. However, tumor-derived exosomes (TEXs), which effectively carry tumor-associated antigens (TAAs) and trigger stronger antigen-specific tumor immunity against autologous tumors than against other tumors, have been widely viewed as attractive potential vaccines for tumor treatment, although improvements are needed. Therefore, in our study, we determined whether RenCa cell-derived exosome (RDE)-stimulated CD8+ T cells exert a stronger specific cytotoxic effect on autologous tumor cells than on other types of tumor cells through the Fas ligand (FasL)/Fas signaling pathway, and whether the combination of RDE-stimulated CD8+ T cells with GM-CSF and IL-12 enhances the anticancer effect. The results showed that RDEs were isolated, as expected, and promoted an increased percentage of CD8+/CD4+ T cells. RDE-stimulated CD8+ T cells also more effectively facilitated cytotoxicity against RenCa cells when combined with GM-CSF and IL-12 *in vitro*. Furthermore, immunization with RDEs restrained the growth of RenCa tumors in mouse models, and facilitated the stimulation of a stronger specific cytotoxic CD8+ T cell response via the FasL/Fas signaling pathway *in vitro*. However, these results were observed less frequently for other types of tumor cells after treatment with RDEs, suggesting that RDEs depend on their antigen specificity to trigger antitumor immune responses. These findings revealed that RDE-stimulated CD8+ T cells combined with GM-CSF and IL-12 can more effectively exert a stronger cytotoxic effect than RDEs alone and that RDEs can induce immunization more effectively against renal cortical adenocarcinoma than against other types of cancer. Therefore, according to our study, exosomes are promising potential vaccines, and the combination of exosome-stimulated CD8+ T cells with GM-CSF and IL-12 may be a novel strategy for the treatment of RCC.

Correspondence to: Professor Yao Zhang, Department of Urology, The First Affiliated Hospital, Chongqing Medical University, 1 Yi Xue Yuan Road, Chongqing 400016, P.R. China
E-mail: zhangyao7407@126.com

Key words: renal cell carcinoma, exosomes, CD8+ T cells, GM-CSF, IL-12, cytotoxicity, immunotherapy

Introduction

The incidence of RCC is increasing worldwide. RCC accounts for approximately 2-3% of tumor diagnoses and tumor mortality cases worldwide; most RCC cases are resistant to traditional radiotherapy and chemotherapy and follow an unpredictable disease course (1,2). In recent years, great progress has been made in the diagnosis and treatment of RCC, although the prognosis remains unsatisfactory. To achieve a better therapeutic effect, early anticipation or identification of patients with aggressive disease or poor prognosis is urgently needed. More importantly, a more efficient and safer therapeutic strategy for eliminating RCC is required to prevent relapse.

One general characteristic of tumor cells is the secretion of membrane microvesicles, which are called exosomes. Exosomes, especially tumor-derived exosomes (TEXs), which are membrane-bound extracellular vesicles 30-100 nm in size secreted by all tumor cells (3), have attracted considerable attention as potential tools for diagnosing cancer and delivering therapeutic anti-cancer drugs (4,5). However, some studies have shown that TEXs alone are less efficient in promoting T cell activation, and may even induce T cell apoptosis; moreover, tumor progression is enhanced and immune escape is promoted due to the expression of immunosuppressive mediators, such as FasL, TNF-associated apoptosis inducing ligand (TRAIL) (6), programmed death-ligand 1 (PD-L1) (7), transforming growth factor-β (TGF-β) (8-11) and HSP72 (12). TEXs are highly enriched in tumor-associated antigens (TAAs) and a series of immune-associated proteins involved in antigen presentation, such as major histocompatibility complex (MHC) molecules (13), inducible co-stimulatory molecules (ICOS) (14) and heat shock proteins (HSP) (15). Functional analyses have demonstrated that TEXs can trigger potent CD8+ T cell-dependent antitumor responses and induce

antitumor immunity via the transfer of exosomal molecules to dendritic cells (DCs) (5,16-18). Therefore, TEXs are an attractive potential vehicle for immunotherapeutics due to their positive role in intercellular communication.

Cytotoxic T cells (CTLs) can mediate their lytic effects through the Fas ligand (L)-Fas pathway, in which the interaction between FasL expressed on CTLs and Fas expressed on target cells triggers apoptosis of the target cells (19). Notably, not all tumor cells, including RenCa cells, express high levels of the Fas protein on the cell surface; this expression is necessary for stimulated CTL-mediated killing (20). CTLs initially recognize target cells through the T cell receptor (TCR) and then strongly adhere to these cells via accessory molecules. After the TCR engages antigenic peptides presented by MHC molecules on target cells, CTLs ultimately induce apoptosis via the interaction between FasL and Fas proteins (21). However, it remains unknown whether RenCa cell-derived TAA-stimulated CTLs induce the FasL/Fas pathway on the surface of other types of tumor cells. Therefore, whether this process of recognition and apoptosis is antigen-specific requires further investigation.

Previous reports showed that TEX-stimulated $CD8^+$ T cells exhibit stronger cytotoxicity and more efficient antitumor immunity against autologous tumor cells than against other types of tumor cells due to the presentation of immune-associated proteins (16-18). Our pre-experimental study found that RCC-associated antigen G250, which is highly expressed in renal cancer-derived exosomes and has limited expression in normal tissue, may play an important role in antigen-specific antitumor immunity (22). However, in general, few previous studies have investigated the cytotoxicity of RDE-stimulated $CD8^+$ T cells. Therefore, in this study, for further verification, exosomes derived from RenCa cell supernatants after 48 h of culture without fetal bovine serum (FBS) were isolated and characterized, and the activating effect of RDEs combined with GM-CSF and IL-12 on $CD8^+$ T cells and the subsequent cytotoxicity of RDE-stimulated $CD8^+$ T cells was also determined. Finally, the potent antigen-specific immunity mediated by RDE-stimulated $CD8^+$ T cells against RenCa cells in comparison with other types of tumor cells were investigated using a variety of methods both *in vivo* and *in vitro*.

Materials and methods

Mice. A total of 200 six-to-eight-week-old (17.40-20.25 g) BALB/c mice were supplied by the Animal Experimental Center of Chongqing Medical University (Chongqing, China) and housed under standard laboratory conditions in the Laboratory Animal Care Facility of Chongqing Medical University (Chongqing, China). Animal care was provided in accordance with institutional guidelines, and all experimental protocols involving animals were performed using a protocol approved by the Ethics Committee of Chongqing Medical University.

Cell lines and culture. The mouse renal cortical adenocarcinoma RenCa cell line, mouse breast cancer 4T1 cell line, and mouse colon cancer CT26 cell line were purchased from Shanghai Cell Bank (Shanghai, China). The cells were cultured in RPMI-1640 medium (Gibco; Thermo Fisher Scientific, Inc. Waltham, MA, USA) supplemented with 10% FBS (Gibco; Thermo Fisher Scientific, Inc.) and 1% penicillin and streptomycin (Gibco; Thermo Fisher Scientific, Inc.) in an incubator with a humidified atmosphere of 5% CO_2 at 37˚C. When the RenCa cells had grown to 80-90% confluency in the plates, the supernatants were harvested for the isolation of RDEs after 48 h of culture without FBS.

Isolation of RDEs. RDEs were extracted and purified as described previously (22). Briefly, culture supernatants were collected and successively centrifuged at 300 x g for 10 min, 800 x g for 30 min, and 10,000 x g for 30 min, after which cells and debris were removed (Ultracentrifuge CP100WX; Hitachi Koki Himac, NuAire, Tokyo, Japan). After concentration by ultrafiltration using a 100 kDa molecular weight cutoff (MWCO) Centriplus centrifugal ultrafiltration tube (EMD Millipore, Billerica, MA, USA) at 1,000 x g for 30 min, the exosome-enriched ultrafiltrate was added to a 30% sucrose/D2O density cushion (Tenglong Weibo Technology, Qingdao, China), followed by ultracentrifugation at 100,000 x g for 60 min at 4˚C. The bottom of the cushion was collected and diluted with phosphate-buffered saline (PBS). The exosomes were further concentrated by centrifugation for 30 min at 1,000 x g in 100 kDa MWCO Amicon Ultra-15 ultrafiltration tubes (EMD Millipore). The collected fluid passed through a membrane filter (0.22 μm) for sterilization, and the exosome sample was stored at -80˚C.

Electron microscopy. The BCA method (Beyotime Institute of Biotechnology, Shanghai, China) was used to quantify the total protein in the RDEs. After quantification, a 20 μl drop of the suspension was loaded onto an electron microscopy grid. Heavy metal staining was performed with 2% phosphotungstic acid (pH 6.8) for 1 min and the morphological characteristics of the RDEs were visualized and observed under a transmission electron microscope (TEM) (JEM-2010, Jeol Ltd., Tokyo, Japan).

Flow cytometry. RDEs and PBS were injected into BALB/c mice via the caudal vein at 10 μg/mouse and 200 μl/mouse per injection, respectively, a total of three times per week for 4 weeks. For tumor inoculation, 200 μl of PBS containing $2x10^6$ RenCa cells was injected subcutaneously into the right flanks of the mice. The mice were sacrificed under deep inhalation anesthesia (2-3% isoflurane; Zhenzhun Institute of Biotechnology, Shanghai, China) and local analgesia (oxybuprocaine hydrochloride; Zhenzhun Institute of Biotechnology) for isolation of splenocytes and tumor single cell suspensions one day after the last injection. Splenocytes and tumor single cell suspensions were generated from mice subjected to three different treatments on days 10, 20 and 30, as described previously (23,24). In brief, erythrocyte-free single cell suspensions were acquired by grinding the spleens several times in RPMI-1640 and incubating with red blood cell lysis buffer (Beyotime Institute of Biotechnology) on ice for 5 min. Tumor biopsies were cut into several small fragments (2-3 mm in length) and placed in an enzyme digest mix consisting of 3,000 U/ml DNAse, 10 mg/ml collagenase and 10 mg/ml hyaluronidase (all from Sigma-Aldrich; Merck Millipore, Darmstadt, Germany) at 37˚C for 2 h. Splenocytes and tumor single cell suspensions were collected, After several

washes, membrane markers of T cell subsets were stained with anti-CD3-APC (Miltenyi Biotec, Bergisch Gladbach, Germany), anti-CD4-FITC (Miltenyi Biotec) and anti-CD8-PE (Miltenyi Biotec) antibodies. Then, the proportions of $CD3^+$, $CD4^+$ and $CD8^+$ T cells in splenocytes and tumor single cell suspensions were analyzed using flow cytometry (Beckman Coulter, Pasadena, CA, USA).

IFN-γ measurements. Next, the mice were divided into three groups and vaccinated intravenously (i.v.) three times per week for 2 weeks. For each injection, three groups of mice received 5 μg RDEs/mouse, 10 μg RDEs/mouse and 200 μl PBS/mouse, respectively. Two weeks after the last immunization, splenic $CD8^+$ T cells from PBS- or RDE-immunized mice were sorted by magnetic beads (Miltenyi Biotec) according to the manufacturer's protocol and as previously described (24), seeded at a concentration of $2.0x10^6$ cells per well in 24-well plates and incubated for 48 h at 37˚C. After incubation, the culture supernatants were collected for cytokine detection. IFN-γ levels in the culture supernatants were measured by enzyme-linked immunosorbent assays (ELISAs) using a commercial kit (R&D Systems, Minneapolis, MN, USA) based on the manufacturer's instructions.

Proliferation assay for $CD8^+$ T cells. Splenocytes from the mice were harvested and depleted of red blood cells. Then, $CD8^+$ T cells were sorted using magnetic beads according to the manufacturer's protocol as previously described (24). The isolated $CD8^+$ T cells were resuspended in PBS at a concentration of $1x10^7$ cells/ml and labeled with 2.5 μM CFSE (Macklin Biochemical Co., Ltd., Shanghai, China) for 10 min at room temperature in the dark. After quenching CFSE with five volumes of RPMI-1640 medium containing 10% FBS and washing several times with PBS containing 2% FBS, $CD8^+$ T cells at a concentration of $1x10^6$ cells/ml were co-cultured with 100 μl of PBS, 5 μg/ml phytohemagglutinin (PHA) (Sigma-Aldrich; Merck Millipore), 5 μg/ml PHA+20 μg/ml RDEs, 20 ng/ml GM-CSF (PeproTech, Shanghai, China), 20 ng/ml IL-12 (PeproTech), 5 μg/ml PHA+20 μg/ml RDEs+20 ng/ml GM-CSF, 5 μg/ml PHA+20 μg/ml RDEs+20 ng/ml IL-12 and 5 μg/ml PHA+20 μg/ml RDEs+20 ng/ml GM-CSF+20 ng/ml IL-12 for a period of 48 h. The cultured cells were harvested, and the proliferation of $CD8^+$ T cells was evaluated by flow cytometry. The supernatant was harvested and analyzed for the release of IFN-γ.

Tumor growth assays. The RenCa cell line, 4T1 cell line, and CT26 cell line were prepared for injection from cultures grown to nearly 95% confluence. The mice were randomly divided into groups, and the three types of tumor cells were enumerated, adjusted to a concentration of ~$2x10^6$ in 200 μl of PBS as described, and injected subcutaneously into the right flanks of the mice to generate three different kinds of tumor model. Then, the mice from the experimental group and the control group were vaccinated three times per week for 4 weeks. For each injection, each mouse in the experimental group received 10 μg of RDEs via the caudal vein and 200 μl of PBS alone as a control. Tumor volume was measured by caliper every three days and calculated according to the formula $V=\pi/6xLxW^2$ (L, length; W, width). The mice were sacrificed under deep inhalation anesthesia (2-3% isoflurane) and local analgesia (oxybuprocaine hydrochloride) for the isolation of tumor tissues.

Cytotoxicity assays. BALB/c mice were i.v. immunized with RDEs and PBS. Seven days later, the spleens were ground, and an erythrocyte dissolving agent was used to acquire splenocyte single cell suspensions after the final stimulation. To perform *in vitro* $CD8^+$ T cell assessments, erythrocyte-free single cell suspensions were sorted by magnetic beads to obtain $CD8^+$ T cells according to the manufacturer's protocol. Next, the isolated $CD8^+$ T cells were re-stimulated with irradiated RenCa cells (4,000 rads; 40 Gy) in the presence of 20 ng/ml IL-2 (PeproTech, Shanghai, China) *in vitro* for three days. Then, the re-stimulated $CD8^+$ T cells were treated with 20 ng/ml GM-CSF, 20 ng/ml IL-12 or 20 ng/ml GM-CSF in combination with 20 ng/ml IL-12 for 48 h. PBS-treated $CD8^+$ T cells were treated with 20 ng/ml GM-CSF or 20 ng/ml IL-12.

Following five days of treatment, the $CD8^+$ T cells derived from different treatments were harvested as effector cells and RenCa cells were used as target cells to establish a co-culture system with different E/T (effector/target) ratios for the LDH release assay via a CytoTox96 Non-Radioactive Cytotoxicity Assay Kit (Promega Biological Products, Ltd., Shanghai, China) and E/T=3 for the apoptosis assay via flow cytometry. Subsequently, RDE-stimulated $CD8^+$ T cells were used as new effector cells, whereas 4T1 cells and CT26 cells served as control target cells for the LDH release assay, apoptosis assay and cell cycle analysis. Briefly, co-culture systems were established with different E/T ratios of RDE-stimulated $CD8^+$ T cells and three types of tumor cells at 37˚C for 4 h. For the inhibition of FasL-dependent cytotoxicity, co-cultures (RenCa cells and $CD8^+$ T cells) were treated or not with 10 μg/ml anti-FasL antibody (MFL-3, 555291; BD Bioscience, San Jose, CA) or isotype control (eBioscience, San Diego, CA, USA) and maintained at 37˚C. Specific lysis (%) was calculated as follows: (Experimental LDH release-effector cells-target spontaneous LDH release)/(target maximum LDH release) x100 (10). Then, when E/T=10, the three types of tumor cells were digested by trypsinization (Beyotime Biotechnology, Shanghai, China) and washed several times for apoptosis assays and cell cycle analysis via flow cytometry. Subsequently, CytoFLEX software (Beckman Coulter, CA, USA) was used to analyze the flow cytometry data. The percentage of apoptosis was calculated from early apoptosis (Annexin V^+/PI^-) plus late apoptosis (Annexin V^+/PI^+), and the cell cycle analysis was compared with the S-phase ratio. Each experiment was performed in triplicate.

Western blot analysis. Western blotting was performed as described previously (25). A total of 20 μg of RDEs or crude protein extracted from RenCa cell lysates was fractionated by 10-15% sodium dodecyl sulfate-polyacrylamide gel electrophoresis (SDS-PAGE) and transferred to polyvinylidene difluoride (PVDF) membranes (Millipore). The membranes were blocked in Tris-buffered saline with Tween (TBST) and 5% nonfat milk for 1 h at room temperature. The rabbit anti-mouse HSP70 monoclonal antibody (ab181606; Abcam, Cambridge, MA, USA), rabbit anti-mouse CD63 monoclonal antibody (ab217345; Abcam) and rabbit anti-mouse CD81

monoclonal antibody (ab109201; Abcam) diluted 1:1,000 were added and incubated at 4˚C overnight. The next day, after incubation with the appropriate horseradish peroxidase (HRP)-conjugated goat anti-rabbit secondary antibodies (ab6721; Abcam) (1:5,000 dilution), the bots were then detected using an Odyssey Infrared System (LI-COR Bioscience, Lincoln, NE, USA).

The cell fractions of three types of tumor cells from different treatments and $CD8^+$ T cells from different treatments were prepared, and protein quantification was performed using the BCA method. Equal amounts of protein were separated via 10-15% SDS-PAGE and transferred to PVDF membranes. The membranes were incubated with TBST and 5% non-fat milk to block nonspecific binding at room temperature, and then they were incubated overnight at 4˚C with rabbit anti-mouse FasL polyclonal antibody (ab15285; Abcam) (for $CD8^+$ T cells), rabbit anti-mouse Fas polyclonal antibody (ab82419; Abcam) (for tumor cells) and rabbit anti-mouse β-actin polyclonal antibody (ab8227; Abcam) (1:1,000 dilution). The next day, after incubation with the HRP-conjugated goat anti-rabbit secondary antibodies (1:5,000 dilution), the immunoassociated protein bands on the membrane were visualized using a chemiluminescence kit (Beyotime Biotechnology, Shanghai, China) and detected using an Odyssey Infrared System. The density of each band was normalized to its loading control (β-actin).

Statistical analysis. All experiments were performed at least three times in triplicate, and all data represent the mean ± SEM. One-way ANOVA or two-way ANOVA followed by Tukey's test was used to analyze the data. Statistical analysis was performed using GraphPad Prism software 7.0 for Mac (GraphPad Software, Inc., San Diego, CA, USA).

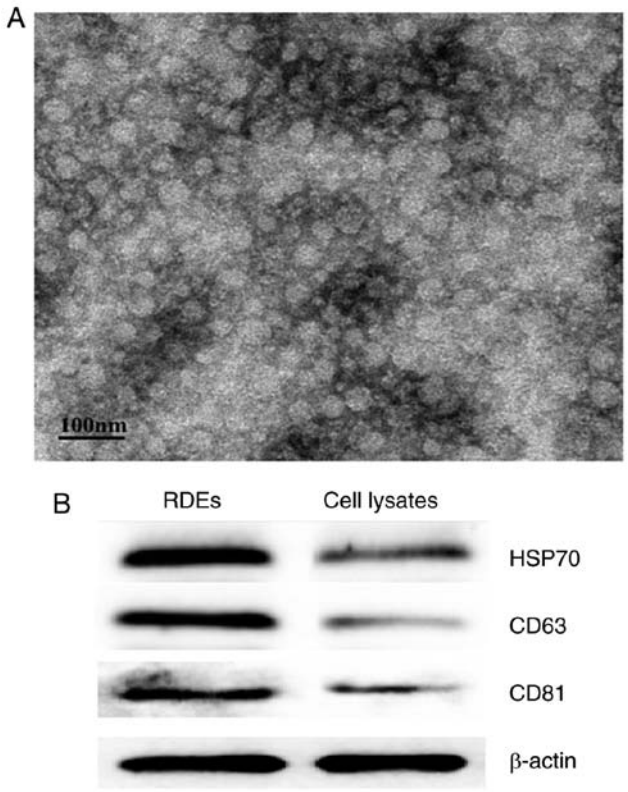

Figure 1. Identification of RDEs. (A) Electron microscopy results showing exosomal membrane-bound spherical vesicles isolated from RenCa cells. Purified RDEs were observed by TEM after ultrafiltration centrifugation and sucrose gradient ultracentrifugation. The exosomes are dimpled microvesicles, ranging from 30-100 nm. The scale bar is 100 nm. (B) Western blot analysis of the expression of proteins, such as HSP70, CD63 and CD81, in RDEs and cell lysates from RenCa cells. RDEs, RenCa cell-derived exosomes; TEM, transmission electron microscopy; HSP70, heat shock protein 70; CD, cluster of differentiation.

Results

Isolation and characterization of RDEs. Whether RenCa cells produce and secrete exosomes was determined by TEM (Fig. 1A). We first isolated and purified exosomes from the culture supernatants of RenCa cells by ultrafiltration and sucrose density gradient centrifugation. Subsequently, the RDEs exhibited the expected morphology and were visualized as spherical membrane-bound vesicles with a diameter of 30-100 nm as determined by TEM. In addition, the western blot analysis results showed that the molecular markers HSP70, CD63 and CD81 were highly expressed in RDEs but relatively rare in the lysates of RenCa cells (Fig. 1B).

RDEs alter T cell subset ratios and stimulate $CD8^+$ T cells. Exosomes from tumor cells have been shown to either suppress or stimulate the immune response (26). Because exosomes have complex immune functions due to their composition, we initiated the study by detecting T cell subset ratios ($CD3^+$ $CD4^+$ and $CD8^+$) in splenocytes from RDE-immunized mice and tumor single cell suspensions from PBS-treated mice via flow cytometry at different time points. An examination of the T cell subset ratios in splenocytes (Fig. 2C and D) from RDE-immunized mice indicated a significant increase in the ratio of $CD8^+/CD4^+$ T cells compared with that of the PBS treatment group, although no difference was observed in the number of $CD3^+$ T cells in the splenocytes (Fig. 2A and B) on days 10, 20 and 30. However, the $CD3^+$ T cells in splenocytes (Fig. 2A and B) from the tumor-bearing mice were significantly decreased. We also found that the proportion of $CD8^+/CD4^+$ T cells in RenCa tumor tissues gradually increased with tumor progression (Fig. 2E and F). To further investigate the immune response induced by RDEs, the levels of IFN-γ in culture supernatants of splenic $CD8^+$ T cells obtained from RDE-immunized mice were measured via an ELISA kit, according to the manufacturer's instructions. As shown in Fig. 2G, compared with $CD8^+$ T cells from PBS-immunized mice, RDEs induced splenic $CD8^+$ T cells obtained from RDE-immunized mice to produce a large amount of IFN-γ.

RDEs combined with GM-CSF and IL-12 promoted the proliferation of $CD8^+$ T cells more effectively than RDEs alone with GM-CSF or IL-12 in vitro. To investigate whether RDE immunization could induce the proliferation of $CD8^+$ T cells effectively *in vitro*, we initiated the study by determining the effect of RDEs on the proliferation rate of $CD8^+$ T cells. Splenic $CD8^+$ T cells obtained from the mice were labeled with CFSE and stimulated with PBS, PHA, PHA+RDEs, GM-CSF, IL-12, PHA+RDEs+GM-CSF, PHA+RDEs+IL-12 and PHA+RDEs+GM-CSF+IL-12. As shown in Fig. 3A and B, the proliferation index of $CD8^+$ T cells was significantly enhanced

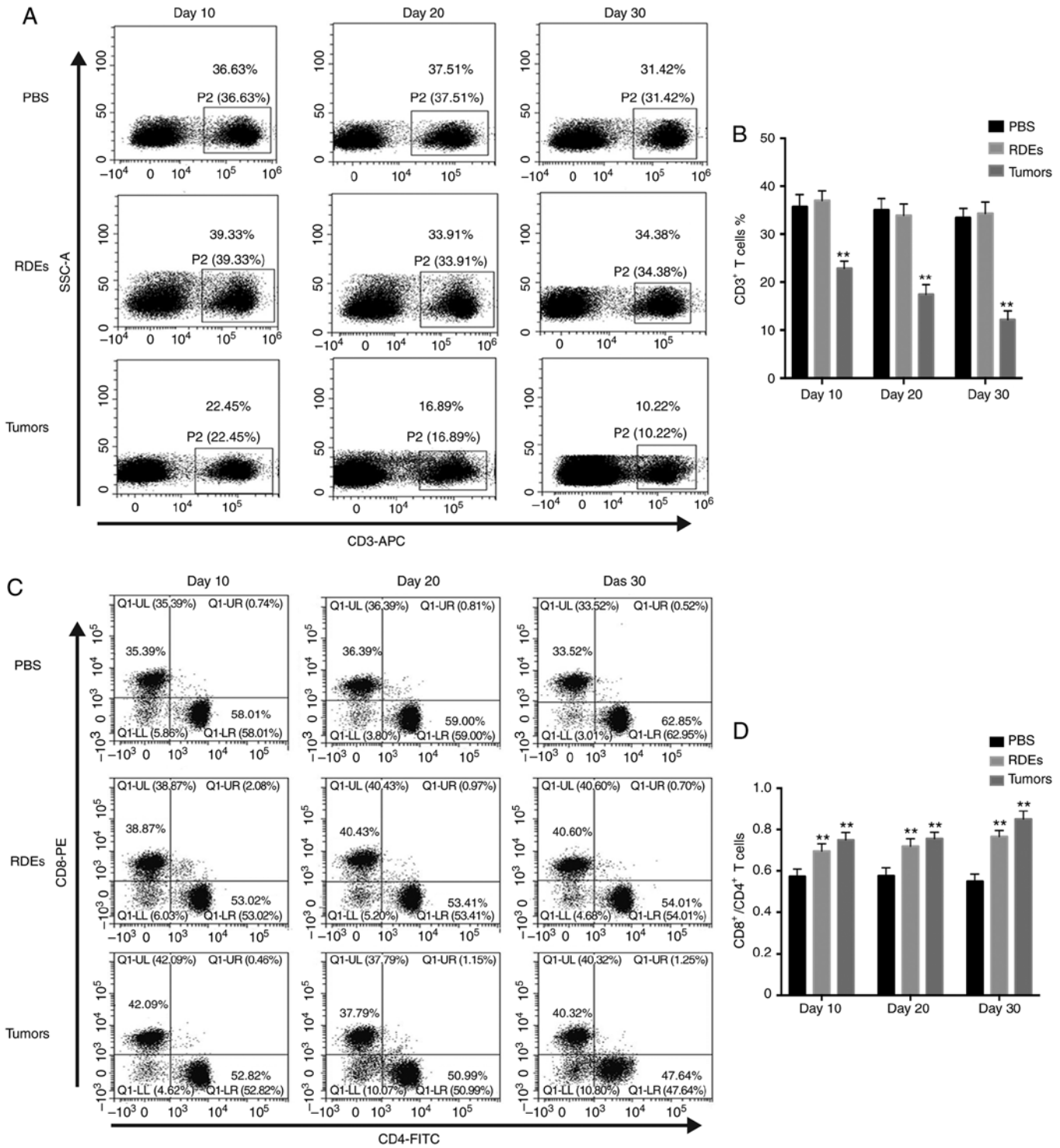

Figure 2. Evaluation of the immune properties of RDEs. Seven-week-old BLAB/c mice were immunized intravenously with PBS and RDEs three times per week for 4 weeks, and RenCa cells were simultaneously injected subcutaneously to generate a tumor-bearing mouse model. One day after a 10-, 20- or 30-day immunization with RDEs, splenocytes without erythrocytes and tumor single-cell suspensions were isolated from mice in the different treatment groups to determine the percentages of T cell subsets [(A and B) $CD3^+$ T cells in splenocytes, (C and D) $CD8^+/CD4^+$ T cells in splenocytes in tumor single cell suspensions] via flow cytometry. Similar data were obtained from three independent experiments. Asterisks indicate significant differences ($^{**}P<0.01$). RDEs, RenCa cell-derived exosomes; CD, cluster of differentiation; IFN-γ, interferon-γ; ELISA, enzyme-linked immunosorbent assay; APC, allophycocyanin; FITC, fluorescein isothiocyanate; PE, phycoerythrin; SSC-A, side scatter area.

by stimulation with PHA compared with PBS; enhanced by stimulation with PHA+RDEs compared with PHA; enhanced by stimulation with GM-CSF or IL-12 compared with PBS; and enhanced by stimulation with PHA+RDEs+GM-CSF or PHA+RDEs+IL-12 compared with PHA+RDEs. The maximum proliferative index was observed in $CD8^+$ T cells stimulated with PHA+RDEs+GM-CSF+IL-12.

To further investigate the ability of RDEs to induce the release of IFN-γ by $CD8^+$ T cells, the cell supernatants of the different treatments described above were harvested and

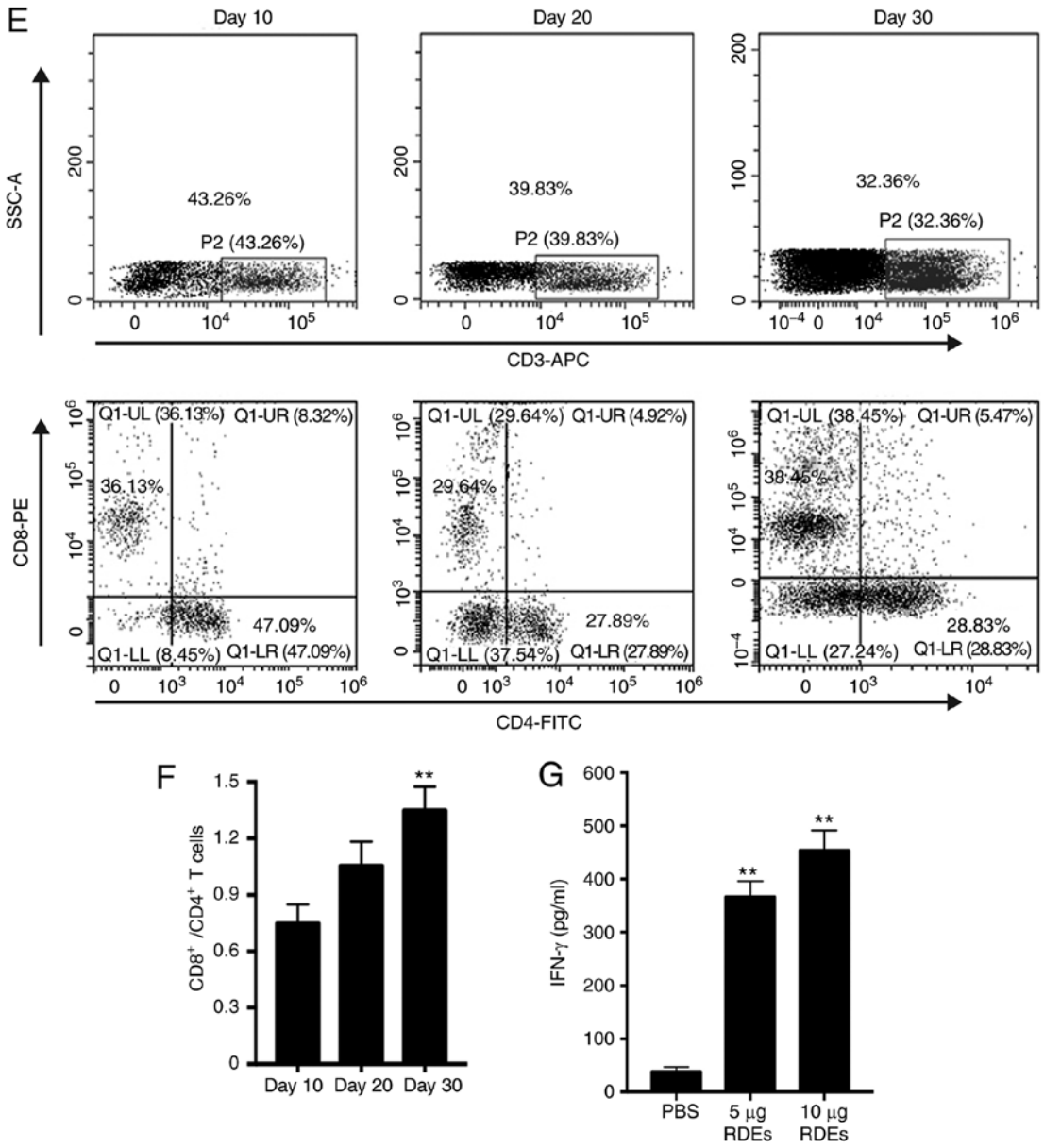

Figure 2. Continued. Evaluation of the immune properties of RDEs. Seven-week-old BLAB/c mice were immunized intravenously with PBS and RDEs three times per week for 4 weeks, and RenCa cells were simultaneously injected subcutaneously to generate a tumor-bearing mouse model. One day after a 10-, 20- or 30-day immunization with RDEs, splenocytes without erythrocytes and tumor single-cell suspensions were isolated from mice in the different treatment groups to determine the percentages of T cell subsets [(E and F) $CD8^+/CD4^+$ T cells in tumor single cell suspensions] via flow cytometry. (G) Splenic $CD8^+$ T cells obtained from mice immunized with PBS and RDEs were incubated under a humidified atmosphere of 5% CO_2 at 37˚C *in vitro*. After 48 h, the supernatants were cleared of dead cells and cell debris, collected and utilized for ELISA to measure the quantity of IFN-γ secreted from RDE-stimulated splenic $CD8^+$ T cells. Similar data were obtained from three independent experiments. Asterisks indicate significant differences ($^{**}P<0.01$). RDEs, RenCa cell-derived exosomes; CD, cluster of differentiation; IFN-γ, interferon-γ; ELISA, enzyme-linked immunosorbent assay; APC, allophycocyanin; FITC, fluorescein isothiocyanate; PE, phycoerythrin; SSC-A, side scatter area.

subjected to an IFN-γ release assay by ELISA. The results demonstrated that RDEs induced the production of IFN-γ by $CD8^+$ T cells *in vitro*, and similar results can be observed above (Fig. 3C). This finding indicates that RDEs can effectively promote the proliferation and activation of $CD8^+$ T cells. Furthermore, the combination of RDEs with GM-CSF and IL-12 may also facilitate a stronger positive effect than RDEs alone with GM-CSF or IL-12 on the stimulation and proliferation of $CD8^+$ T cells.

More effective induction of cytotoxic effects in RDE-stimulated $CD8^+$ T cells treated with GM-CSF and IL-12. To explore whether RDE-stimulated $CD8^+$ T cells combined with GM-CSF and IL-12 could induce more potent cytotoxic effects, we harvested RDE-stimulated $CD8^+$ T cells treated with GM-CSF, IL-12 or GM-CSF in combination with IL-12 to establish a co-culture system with different E/T ratios. GM-CSF, IL-12-treated $CD8^+$ T cells served as the control. The results (Fig. 4A) showed that RDE-stimulated $CD8^+$ T cells treated with GM-CSF or IL-12 could kill RenCa cells more effectively than RDE-stimulated $CD8^+$ T cells alone, and GM-CSF in combination with IL-12 could achieve the maximum cytotoxic effect. However, GM-CSF or IL-12 alone failed to increase the cytotoxic effect of control $CD8^+$

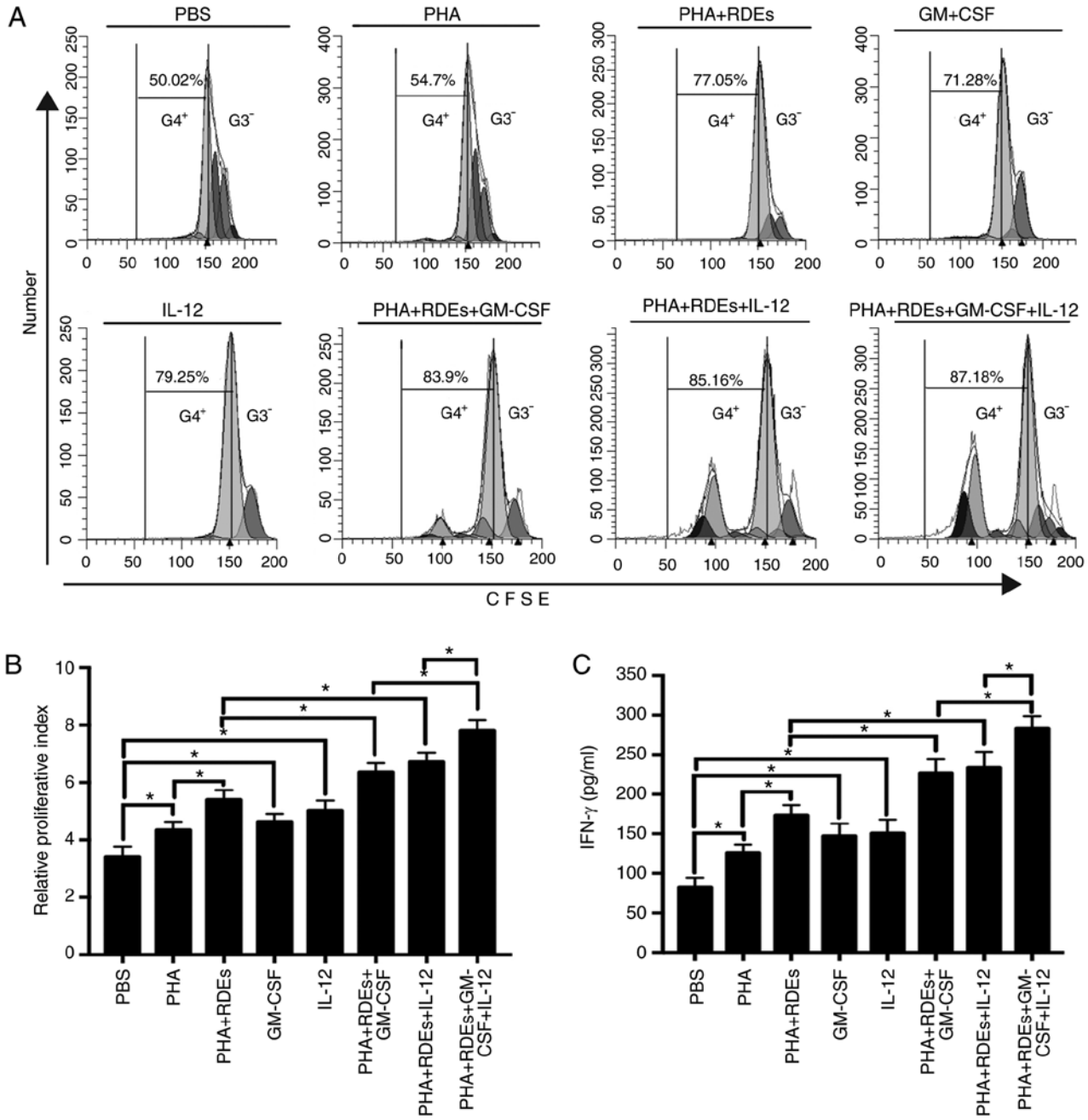

Figure 3. RDEs combined with GM-CSF and IL-12 induce the proliferation and stimulation of CD8+ T cells more effectively than RDEs alone with GM-CSF or IL-12 *in vitro*. Splenic CD8+ T cells were labeled with CFSE and treated with PBS, PHA, PHA+RDEs, GM-CSF, IL-12, PHA+RDEs+GM-CSF, PHA+RDEs+IL-12 and PHA+RDEs+GM-CSF+IL-12 for 48 h. (A) Number of cell divisions was assessed by successive halving of the fluorescence intensity of CFSE by flow cytometry. RDE-treated CD8+ T cells exhibited a smaller number of cells with lower (G1, G2 and G3) cell divisions and a greater number of cells with higher (G4+) cell divisions than non-RDE-treated CD8+ T cells. The application of GM-CSF and IL-12 enhanced this effect. (B) Relative proliferation index of each treatment group was also assessed by flow cytometry. (C) Supernatants of different treatment groups were harvested, and the release of IFN-γ was determined by ELISA. Each group was tested in triplicate wells, and the values were statistically analyzed by one-way ANOVA (*P<0.05). RDEs, RenCa cell-derived exosomes; ELISA, enzyme-linked immunosorbent assay; IFN-γ, interferon-γ; GM-CSF, granulocyte-macrophage colony stimulating factor; G1-4, generation 1-4; IL-12, interleukin-12; PHA, phytohemagglutinin; CFSE, carboxyfluorescein diacetate succinimidyl ester; ANOVA, analysis of variance; CD, cluster of differentiation.

T cells. Similar results were observed when flow cytometry was used to measure the proportion of apoptotic RenCa cells when E/T=3 (Fig. 4B and C). The results demonstrated the antitumor effects of RDE-stimulated CD8+ T cells combined with GM-CSF and IL-12.

RDEs specifically inhibit the growth of RenCa tumors. To determine whether RenCa tumors were more affected by RDEs than other types of tumors, we used RDEs and PBS to treat BALB/c mice bearing established subcutaneous RenCa, 4T1 and CT26 tumors and followed the tumor growth. Tumor size was measured using calipers, and overall survival was monitored and recorded. As shown in Fig. 5A and D, compared with PBS, RDE vaccination promoted a marked inhibition of RenCa tumor growth. In addition, a phenomenon occurred in which the difference

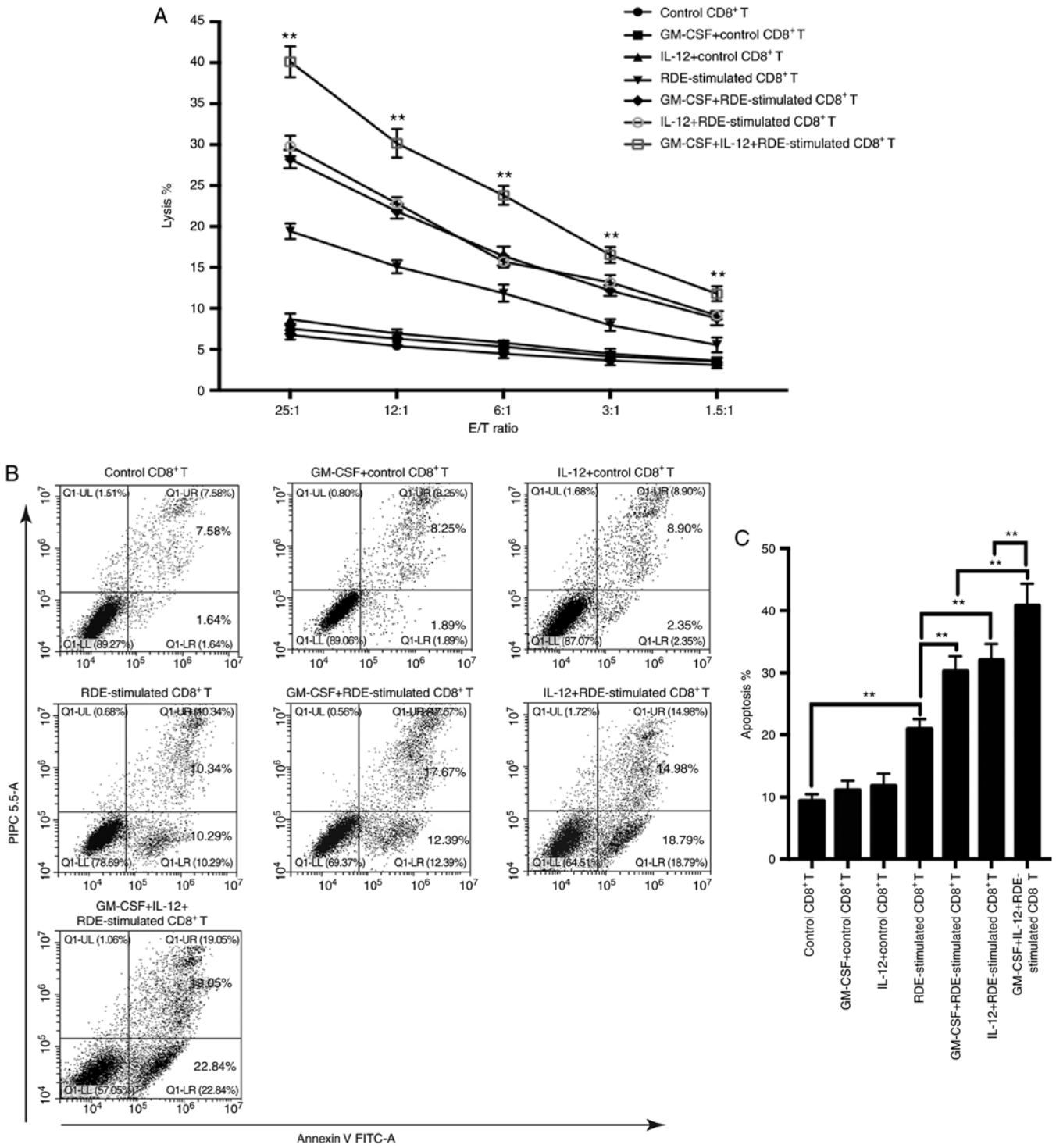

Figure 4. Increased cytotoxicity of RDE-stimulated CD8+ T cells in combination with GM-CSF and IL-12. Splenic CD8+ T cells from immunized mice were re-stimulated with irradiated RenCa cells in the presence of IL-2 *in vitro*. Three days later, re-stimulated CD8+ T cells were treated with GM-CSF, IL-12 and GM-CSF in combination with IL-12 for 48 h. Control CD8+ T cells were treated with GM-CSF or IL-12. CD8+ T cells derived from the different treatments were used as effectors, and the target cells were RenCa cells. (A) Cytotoxic assay of CD8+ T cells was performed using the LDH release assay with the following formula: Lysis (%)=(experimental LDH release-effector cells-target spontaneous LDH release)/(target maximum LDH release) x100. (B and C) Apoptosis analysis was performed when E/T=3, and the proportion of apoptotic RenCa cells was detected by flow cytometry (**P<0.01). IL, interleukin; GM-CSF, granulocyte-macrophage colony stimulating factor; CD, cluster of differentiation; RDEs, RenCa cell-derived exosomes; LDH, lactate dehydrogenase; E/T, effector/target; FITC-A, fluorescein isothiocyanate-area; PI PC 5.5-A, propidium iodide PC 5.5-area.

in tumor growth between the RDE groups and the PBS groups was not observed in mice with 4T1 (Fig. 5B and D) and CT26 (Fig. 5C and D) tumors. Moreover, the survival rate of RenCa tumor-challenged mice was also significantly increased by RDE immunization, although mice with 4T1 and CT26 tumors did not exhibit corresponding differences between treatment groups (Fig. 5E). Taken together, the data indicate that RDEs induced more effective therapeutic immunity against renal cortical adenocarcinoma than against other cancer types.

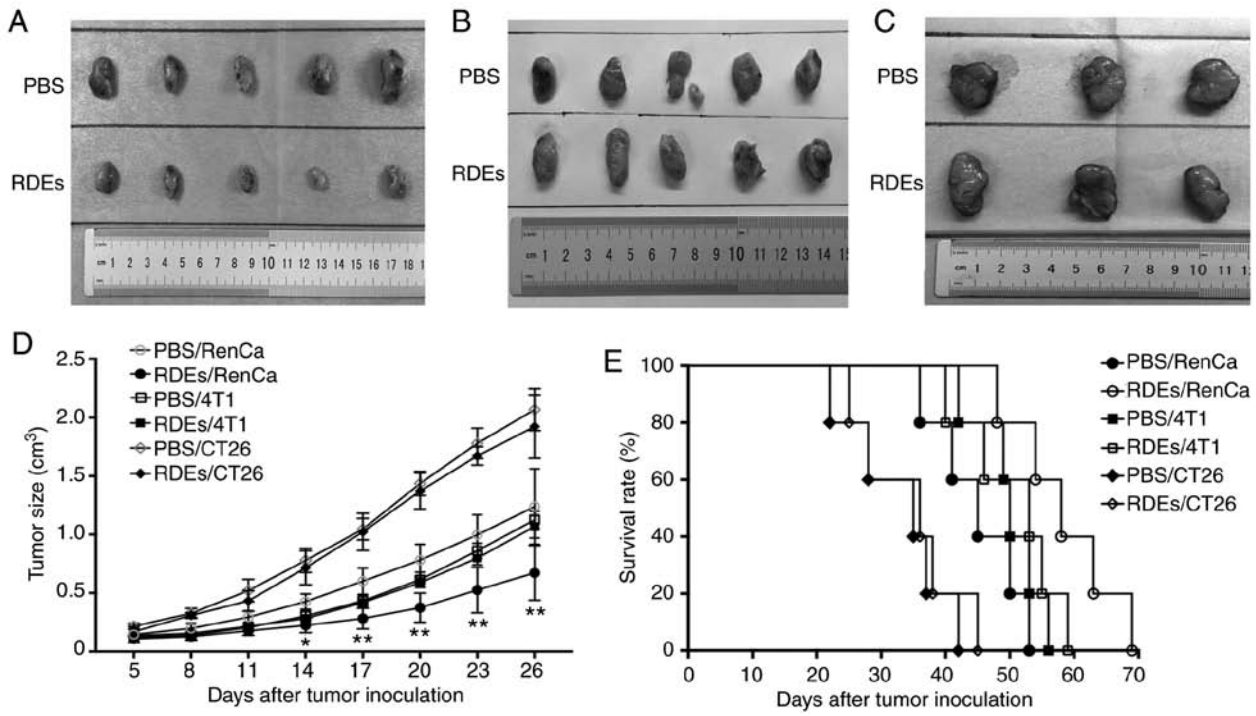

Figure 5. Specific resistance effect of RDEs on RenCa tumor growth. BALB/c mice received a subcutaneous injection of $2x10^6$ tumor cells and an intravenous injection of 10 μg of RDEs or 200 μl of PBS for a total of three treatments per week for nearly 4 weeks. Tumor growth curves and survival curves of RDE-treated mice bearing (A) RenCa tumors, (B) 4T1 tumors and (C) CT26 tumors and the corresponding control groups are shown. (D) Mean ± SD values for tumor size and (E) survival rate showing significant or non-significant differences between tumor-bearing mice treated with RDEs and PBS. The growth of the implanted tumor was measured over a 26-day period, and the survival rate of immunized mice was recorded until the 69th day. Each point represents the mean of the average tumor size (*P<0.05; **P<0.01). RDEs, RenCa cell-derived exosomes; SD, standard deviation.

RDE-stimulated CD8$^+$ T cells induce stronger immunity against renal cancer than against other cancer types in vitro. Next, we investigated the specific cytotoxic effects of RDE-stimulated splenic CD8$^+$ T cells against three types of tumor cells using the LDH release method. Seven days after intravenous immunization with RDEs, splenic CD8$^+$ T cells re-stimulated with irradiated RenCa cells were sorted and co-cultured with different target cells at various E/T ratios. As shown in Fig. 6A, RDE-stimulated CD8$^+$ T cells displayed potent cytotoxic ability against RenCa cells at all E/T ratios, while no detectable CD8$^+$ T response was induced by PBS. A less dramatic increase in the killing rate occurred when 4T1 and CT26 cells were treated with RDE-stimulated CD8$^+$ T cells at E/T ratios over 12:1.

Subsequently, to determine the effect of effector cells on apoptosis and the cell cycle in three types of target cells, the percentage of cells undergoing apoptosis and the cell cycle distribution of target cells were determined and quantified using an apoptosis assay and a cell cycle assay, respectively, via flow cytometry. As shown in Fig. 6C and D, Annexin V-based apoptosis analysis revealed significant increases in the percentages of apoptotic cells in the lower right and upper right quadrants of the histograms, called early and late apoptotic cells, respectively, in RenCa cells treated with RDE-stimulated CD8$^+$ T cells, compared with controls at an E/T ratio of 10:1. By contrast, compared with the controls, there was a less marked increase in the apoptosis rate when 4T1 and CT26 cells were tested with RDE-stimulated CD8$^+$ T cells. Furthermore, in cell cycle assays (Fig. 6B), RenCa cells treated with RDE-stimulated CD8$^+$ T cells showed a significantly decreased S-phase ratio compared with the controls, but the 4T1 and CT26 cells did not, indicating that the killing activity of these RDE-stimulated CD8$^+$ T cells was exosome antigen-specific.

A previous study demonstrated that cytotoxic T cells can mediate their lytic effects through a distinct pathway called the Fas-based pathway, in which the interaction between FasL expressed on CTLs and Fas presented on target cells triggers apoptosis and cell death (20). Hence, in the present study, the expression of FasL on CD8$^+$ T cells and Fas on tumor cells was detected by western blotting. As shown in Fig. 6E, the co-culture of RDE-stimulated CD8$^+$ T cells and RenCa cells resulted in an increase in FasL expression on the CD8$^+$ T cell surface and an increase in Fas expression on RenCa cells, compared with the control levels. However, in other types of tumor cells, similar results were not observed. The perforin inhibitor blocked the majority of RenCa cell CTL lysis, suggesting a major effector role for granule-mediated lysis *in vitro* (21). However, some inhibition of lysis was also observed when the anti-FasL antibody was present (Fig. 6F). These findings suggest that the FasL/Fas-mediated mechanism also plays a significant role in the cytotoxicity of RDE-stimulated CD8$^+$ T cells.

Discussion

Research on exosomes has attracted substantial attention since their initial discovery. TEXs are not only involved in establishing a favorable microenvironment surrounding the tumor but also induce a comprehensive alteration of the immune system (27,28).

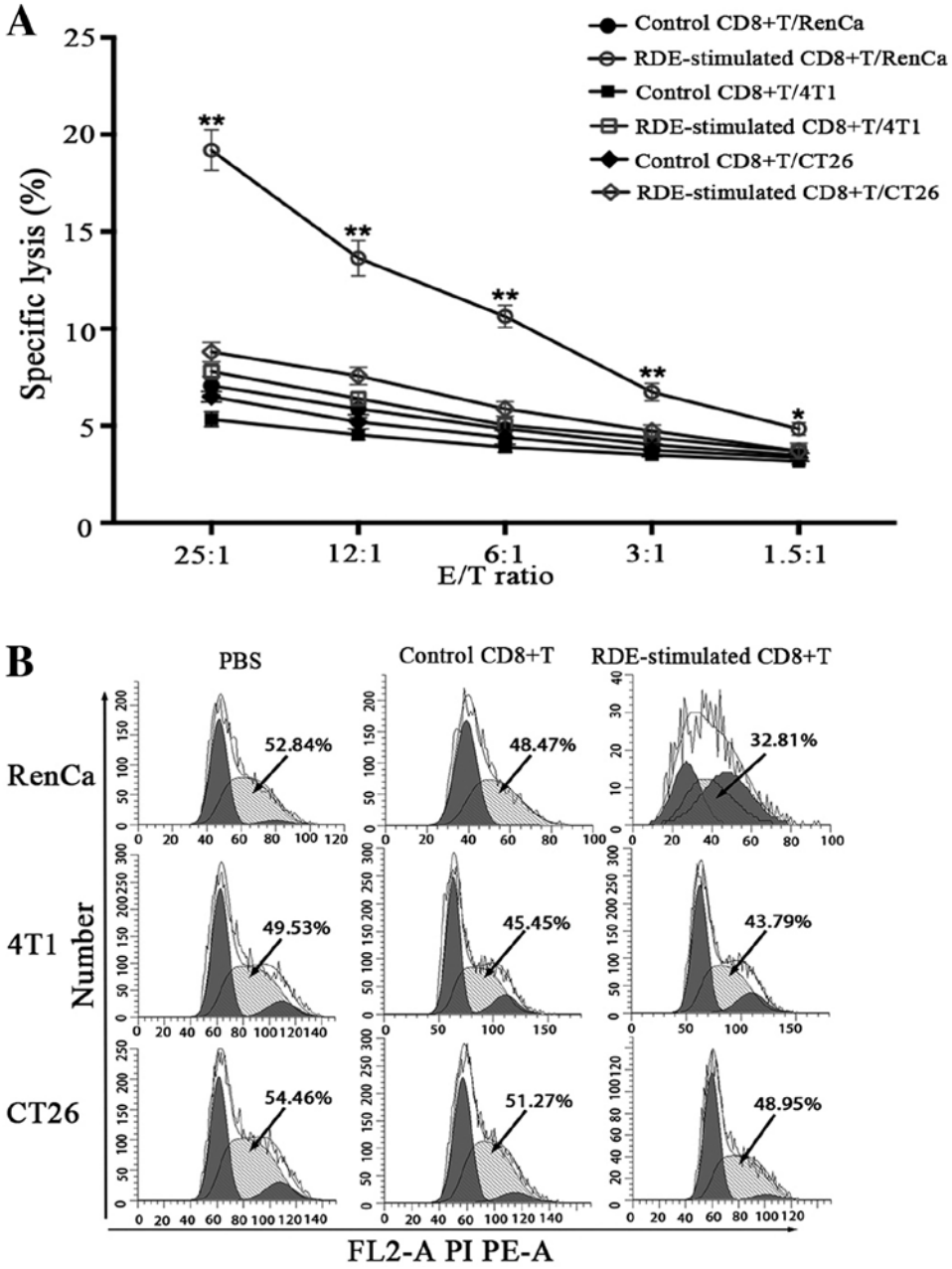

Figure 6. Development of antigen-specific CD8$^+$ T cell cytotoxic activity *in vitro*. (A) Splenic CD8$^+$ T cells from immunized mice were re-stimulated with irradiated RenCa cells in the presence of IL-2 *in vitro*. Three days later, stimulated CD8$^+$ T cells were harvested and used as effector (E) cells in the LDH release assay, whereas RenCa cells or control 4T1 and CT26 cells were used as the target (T) cells and mixed with effector cells at different ratios. Specific lysis (%) was calculated with the following formula on the basis of the amount of LDH release: (Experimental LDH release-effector cells-target spontaneous LDH release)/(target maximum LDH release) x100. RDE-stimulated CD8$^+$ T cells and control CD8$^+$ T cells were co-cultured with three types of tumor cells at a 10:1 ratio. (B) Cell cycle distribution of the three types of tumor cells were detected by flow cytometry. The data are representative of three independent experiments and expressed as the mean ± SD (*P<0.05, **P<0.01). IL, interleukin; CD, cluster of differentiation; RDEs, RenCa cell-derived exosomes; FITC-A, fluorescein isothiocyanate-area; FL2-A PI PE-A, FL2-A propidium iodide PE 5.5-area; PI PC 5.5-A, propidium iodide PC 5.5-area; SD, standard deviation; LDH, lactate dehydrogenase; FasL, Fas ligand.

A full understanding of TEX immunization includes the observation that TEXs are a source of shared TAA and stimulatory molecules for the innate immune response, which can induce T cell-dependent immunity in mice or human tumor models under some conditions (8-11,16-18). This property makes TEXs novel potential vaccines for the treatment of tumors. However, according to previous studies, TEXs can be equipped with either immune-stimulatory ability or immunosuppressive ability due to the complexity of their components (26). The immunosuppressive abilities of TEXs have been characterized in numerous cancer types and in the context of several different mediators, such as the amplification of myeloid-derived suppressor cell (MDSC) (23), the induction of effector T cell apoptosis (29,30), the suppression of natural killer (NK) cell capability (31) and the disruption of dendritic cell (DC) differentiation and maturation (32). However, this effect has no negative impact on their availability to transmit TAA to mature DCs and induce an immune-stimulatory response that is superior to their immunosuppressive effect in tumor-bearing hosts. Therefore, we have demonstrated by

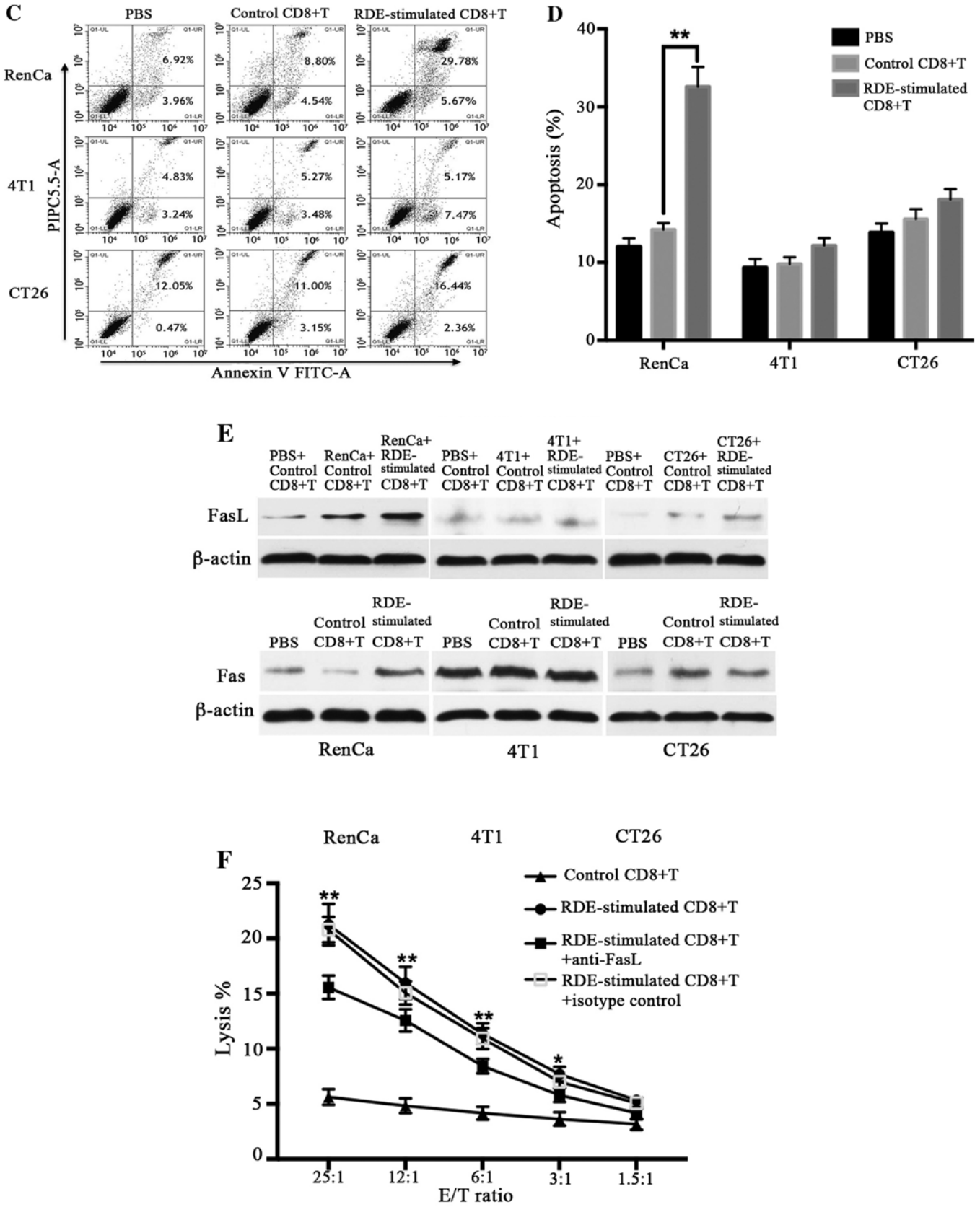

Figure 6. Continued. Development of antigen-specific CD8$^+$ T cell cytotoxic activity *in vitro*. RDE-stimulated CD8$^+$ T cells and control CD8$^+$ T cells were co-cultured with three types of tumor cells at a 10:1 ratio. (C and D) Percentage of apoptosis of the three types of tumor cells was detected by flow cytometry. (E) FasL protein levels on the surface of CD8$^+$ T cells after different treatments and Fas levels on the surface of RenCa, 4T1 and CT26 cells were assessed by western blot analysis. The upper panel and lower panel show histogram analyses of the expression levels of the FasL and Fas proteins, respectively. β-actin was used as an internal control. (F) Cytotoxic assay performed in the presence of anti-FasL antibody or isotype control (10 μg/ml). The data are representative of three independent experiments and expressed as the mean ± SD (*P<0.05, **P<0.01). IL, interleukin; CD, cluster of differentiation; RDEs, RenCa cell-derived exosomes; FITC-A, fluorescein isothiocyanate-area; FL2-A PI PE-A, FL2-A propidium iodide PE 5.5-area; PI PC 5.5-A, propidium iodide PC 5.5-area; SD, standard deviation; LDH, lactate dehydrogenase; FasL, Fas ligand.

means of T cell subset ratio analyses, tumor growth assays, IFN-γ secretion assays, proliferation assays of $CD8^+$ T cells and cytotoxicity assays of RDE-stimulated $CD8^+$ T cells that RDEs express immunologically relevant molecules to induce *in vivo* and *in vitro* immune activation and elicit a potent immune response. Additionally, when RDE-stimulated $CD8^+$ T cells are combined with GM-CSF and IL-12, the immune response is further optimized. Furthermore, we can conclude from the tumor growth assay that in the case of RDEs, their immune-stimulatory ability is greater than their immunosuppressive ability.

Previous studies have reported that the injection of an increasing number of TEXs could provide a source of tumor-rejection antigens relevant for immunization (33) and the crucial components of the immune response are DCs that participate in antigen presentation and mediate antigen specificity of the immune response (34). Therefore, based on the positive effects of RDEs on immune cells, we investigated the specific cytotoxic function of RDE-stimulated splenic $CD8^+$ T cells. As expected, RDE antigen-specific splenic $CD8^+$ T cells displayed stronger cytotoxicity for the autologous tumor cells than the other types of tumor cells at any E/T ratio. *In vitro* experiments have shown that TEXs may need to rely on host DCs for the induction of an immune response (8-11,12-14); however, TEXs can be taken up by $CD8^+$ T cells, although a lack of DC participation was reported in some experiments, and TEXs can directly induce specific killing activity of $CD8^+$ T cells via exosomal MHC molecules (35). Notably, we observed a dramatic phenomenon in which RDE-stimulated $CD8^+$ T cells displayed a slightly weaker lethality for CT26 cells and 4T1 cells. This effect could be caused by nonspecific cytotoxicity or a mixture of RDE-stimulated NK cells that lack specific cytotoxicity for tumor cells among the $CD8^+$ T cells derived from the splenocytes of immunized mice (15).

Two major molecular pathways of $CD8^+$ T cell-regulated cytotoxicity have been proven: i) the exocytosis of granules containing perforin and granzyme molecules and ii) the interaction of FasL on T cells with the apoptosis-inducing Fas molecule on target cells (19). CTLs initially recognize target cells using the TCR and strongly adhere to these cells via accessory molecules; finally, FasL partially transmits death signals to Fas-positive target cells and induces cell apoptosis. These anti-RenCa tumor $CD8^+$ T cells can lyse RenCa cells *in vitro* via the perforin/granzyme and FasL/Fas pathways. Moreover, proinflammatory cytokines, such as IFN-γ and TNF-α could play a key role in the effector phase of the immune response because these cytokines sensitize tumor cells to lysis by both of the above pathways (21). This observation may explain why RDE-stimulated $CD8^+$ T cell-treated RenCa cells highly expressed the Fas protein compared with RenCa cells treated with control $CD8^+$ T cells or PBS. T-cell-mediated cytotoxicity *in vitro* was enhanced via triggering through the crossing-linking of TCR, which is known to be necessary for the up-regulation of cell surface FasL (36). However, similar results were not observed in other types of tumor cells, suggesting that the effect of pro-inflammatory cytokines is based on the specific recognition and combination of FasL and Fas and that apoptosis mediated by the FasL-Fas pathway is characterized by antigenic specificity. However, controlling tumor growth and metastasis using CTLs alone is difficult due to the complex mechanisms of tumor cell proliferation, progression and metastasis. CTLs expressing FasL can induce apoptosis in tumor cells, whereas tumor cells expressing FasL can also induce the elimination of CTLs according to the tumor anti-killing theory (37), which necessitates the optimization of RDE-based vaccines, such as the use of RDE-stimulated $CD8^+$ T cells in combination with GM-CSF and IL-12.

Taken together, these data demonstrate that investigating TEX-associated mechanisms in the context of the immune response is vital for the development of novel therapies. Additional mechanisms that modify TEXs to suppress and evade the immune system have attracted attention. Immunosuppressive mediators that are present in TEXs, such as FasL, TRAIL (6), TGF-β (8-11), PD-L1 (7), and HSP72 (12), can exert adverse effects on the antitumor response. Furthermore, a negative effect of the immunogenicity of TEX-based vaccines arises when TEXs lack the expression of MHC complexes (13), adhesion molecule signals (38) and co-stimulatory molecules (14) that can enhance antitumor immunity. Therefore, extensive research has already demonstrated that downregulating these mediators of immunosuppression and avoiding the absence of these immune-stimulatory factors can lead to a more efficient induction of systemic antitumor immunity and CTL responses. Furthermore, the combination of TEXs with GM-CSF (39) and IL-12 (22) may also facilitate a stronger positive effect on the antitumor response. The activation of NK cells induced by TEXs from one of these tumors may have a relatively weak nonspecific killing effect on other tumors in patients who have two or more tumors simultaneously. In summary, exosome therapy offers a promising immune-based strategy for the development of cancer vaccines; however, we must still optimize the TEX-based treatment program in clinical trials due to the complex role of TEX components in immune regulation.

In conclusion, our study demonstrated that RDEs could be used as vaccines to effectively retard renal cancer growth and prolong survival in mice. RDEs can promote the proliferation and activation of $CD8^+$ T cells, and the combination of RDE-stimulated $CD8^+$ T cells with GM-CSF or IL-2 may achieve a more satisfactory antitumor immune response. Furthermore, RDE-stimulated $CD8^+$ T cells can induce antigen-specific anti-renal cancer effects through the FasL/Fas signaling pathway. Therefore, our study provides a promising therapy for renal cancer using exosome-based antigen-specific vaccines.

Acknowledgements

Not applicable.

Funding

The National Natural Science Foundation of China (grant no. 81272572) provided financial support for this study.

Availability of data and materials

All data generated or analyzed during this study are included in this published article, and are available on reasonable request.

Authors' contributions

HYX conducted experiments, data acquisition and analysis and was a major contributor in writing the manuscript; YZ made a significant contribution to the conception and design of the experiments; NL and NY were involved in cell culture and exosome extraction; XFX, HXW and XYL collected and analyzed the data. All authors read and approved the final manuscript.

Ethics approval and consent to participate

The Ethics Committee of Chongqing Medical University approved this study.

Patient consent for publication

Not applicable.

Competing interests

The authors declare that they have no competing interests, and all authors have confirmed the accuracy of this statement.

References

1. Siegel RL, Miller KD and Jemal A: Cancer statistics, 2017. CA Cancer J Clin 67: 7-30, 2017.
2. Ljungberg B, Cowan NC, Hanbury DC, Hora M, Kuczyk MA, Merseburger AS, Patard JJ, Mulders PF and Sinescu IC; European association of urology guideline group: EAU guidelines on renal cell carcinoma: The 2010 update. Eur Urol 58: 398-406, 2010.
3. Colombo M, Raposo G and Théry C: Biogenesis, secretion, and intercellular interactions of exosomes and other extracellular vesicles. Annu Rev Cell Dev Biol 30: 255-289, 2014.
4. Sundararajan V, Sarkar FH and Ramasamy TS: Correction to: The versatile role of exosomes in cancer progression: Diagnostic and therapeutic implications. Cell Oncol (Dordr) 41: 223-252, 2018.
5. Gu X, Erb U, Büchler MW and Zöller M: Improved vaccine efficacy of tumor exosome compared to tumor lysate loaded dendritic cells in mice. Int J Cancer 136: E74-E84, 2015.
6. Stenqvist AC, Nagaeva O, Baranov V and Mincheva-Nilsson L: Exosomes secreted by human placenta carry functional Fas ligand and TRAIL molecules and convey apoptosis in activated immune cells, suggesting exosome-mediated immune privilege of the fetus. J Immunol 191: 5515-5523, 2013.
7. Chen G, Huang AC, Zhang W, Zhang G, Wu M, Xu W, Yu Z, Yang J, Wang B, Sun H, *et al*: Exosomal PD-L1 contributes to immunosuppression and is associated with anti-PD-1 response. Nature 560: 382-386, 2018.
8. Wieckowski EU, Visus C, Szajnik M, Szczepanski MJ, Storkus WJ and Whiteside TL: Tumor-derived microvesicles promote regulatory T cell expansion and induce apoptosis in tumor-reactive activated $CD8^+$ T lymphocytes. J Immunol 183: 3720-3730, 2009.
9. Valenti R, Huber V, Filipazzi P, Pilla L, Sovena G, Villa A, Corbelli A, Fais S, Parmiani G and Rivoltini L: Human tumor-released microvesicles promote the differentiation of myeloid cells with transforming growth factor-beta-mediated suppressive activity on T lymphocytes. Cancer Res 66: 9290-9298, 2006.
10. Huang F, Wan J, Hao S, Deng X, Chen L and Ma L: TGF-β1-silenced leukemia cell-derived exosomes target dendritic cells to induce potent anti-leukemic immunity in a mouse model. Cancer Immunol Immunother 66: 1321-1331, 2017.
11. Huang F, Wan J, Hu W and Hao S: Enhancement of anti-leukemia immunity by leukemia-derived exosomes via downregulation of TGF-β1 expression. Cell Physiol Biochem 44: 240-254, 2017.
12. Chalmin F, Ladoire S, Mignot G, Vincent J, Bruchard M, Remy-Martin JP, Boireau W, Rouleau A, Simon B, Lanneau D, *et al*: Membrane-associated Hsp72 from tumor-derived exosomes mediates STAT3-dependent immunosuppressive function of mouse and human myeloid-derived suppressor cells. J Clin Invest 120: 457-471, 2010.
13. Yang MQ, Du Q, Varley PR, Goswami J, Liang Z, Wang R, Li H, Stolz DB and Geller DA: Interferon regulatory factor 1 priming of tumour-derived exosomes enhances the antitumour immune response. Br J Cancer 118: 62-71, 2018.
14. Escola JM, Kleijmeer MJ, Stoorvogel W, Griffith JM, Yoshie O and Geuze HJ: Selective enrichment of tetraspan proteins on the internal vesicles of multivesicular endosomes and on exosomes secreted by human B-lymphocytes. J Biol Chem 273: 20121-20127, 1998.
15. Xie Y, Bai O, Zhang H, Yuan J, Zong S, Chibbar R, Slattery K, Qureshi M, Wei Y, Deng Y and Xiang J: Membrane-bound HSP70-engineered myeloma cell-derived exosomes stimulate more efficient CD8(+) CTL- and NK-mediated antitumour immunity than exosomes released from heat-shocked tumour cells expressing cytoplasmic HSP70. J Cell Mol Med 14: 2655-2666, 2010.
16. Bu N, Wu H, Sun B, Zhang G, Zhan S, Zhang R and Zhou L: Exosome-loaded dendritic cells elicit tumor-specific $CD8^+$ cytotoxic T cells in patients with glioma. J Neurooncol 104: 659-667, 2011.
17. Hao S, Bai O, Yuan J, Qureshi M and Xiang J: Dendritic cell-derived exosomes stimulate stronger $CD8^+$ CTL responses and antitumor immunity than tumor cell-derived exosomes. Cell Mol Immunol 3: 205-211, 2006.
18. Yao Y, Chen L, Wei W, Deng X, Ma L and Hao S: Tumor cell-derived exosome-targeted dendritic cells stimulate stronger $CD8^+$ CTL responses and antitumor immunities. Biochem Biophys Res Commun 436: 60-65, 2013.
19. Kreuwel HT, Morgan DJ, Krahl T, Ko A, Sarvetnick N and Sherman LA: Comparing the relative role of perforin/granzyme versus Fas/Fas ligand cytotoxic pathways in $CD8^+$ T cell-mediated insulin-dependent diabetes mellitus. J Immunol 163: 4335-4341, 1999.
20. Sayers TJ, Brooks AD, Lee JK, Fenton RG, Komschlies KL, Wigginton JM, Winkler-Pickett R and Wiltrout RH: Molecular mechanisms of immune-mediated lysis of murine renal cancer: Differential contributions of perforin-dependent versus Fas-mediated pathways in lysis by NK and T cells. J Immunol 161: 3957-3965, 1998.
21. Seki N, Brooks AD, Carter CR, Back TC, Parsoneault EM, Smyth MJ, Wiltrout RH and Sayers TJ: Tumor-specific CTL kill murine renal cancer cells using both perforin and Fas ligand-mediated lysis in vitro, but cause tumor regression in vivo in the absence of perforin. J Immunol 168: 3484-3492, 2002.
22. Zhang Y, Luo CL, He BC, Zhang JM, Cheng G and Wu XH: Exosomes derived from IL-12-anchored renal cancer cells increase induction of specific antitumor response in vitro: A novel vaccine for renal cell carcinoma. Int J Oncol 36: 133-140, 2010.
23. Wang J, De Veirman K, Faict S, Frassanito MA, Ribatti D, Vacca A and Menu E: Multiple myeloma exosomes establish a favourable bone marrow microenvironment with enhanced angiogenesis and immunosuppression. J Pathol 239: 162-173, 2016.
24. Baldan V, Griffiths R, Hawkins RE and Gilham DE: Efficient and reproducible generation of tumour-infiltrating lymphocytes for renal cell carcinoma. Br J Cancer 112: 1510-1518, 2015.
25. Yuan Y, Zhang Y, Zhao S, Chen J, Yang J, Wang T, Zou H, Wang Y, Gu J, Liu X, *et al*: Cadmium-induced apoptosis in neuronal cells is mediated by Fas/FasL-mediated mitochondrial apoptotic signaling pathway. Sci Rep 8: 8837, 2018.
26. Junker K, Heinzelmann J, Beckham C, Ochiya T and Jenster G: Extracellular vesicles and their role in urologic malignancies. Eur Urol 70: 323-331, 2016.
27. Graner MW, Schnell S and Olin MR: Tumor-derived exosomes, microRNAs, and cancer immune suppression. Semin Immunopathol 40: 505-515, 2018.
28. Barros FM, Carneiro F, Machado JC and Melo SA: Exosomes and immune response in cancer: Friends or foes? Front Immunol 9: 730, 2018.
29. Ludwig S, Floros T, Theodoraki MN, Hong CS, Jackson EK, Lang S and Whiteside TL: Suppression of lymphocyte functions by plasma exosomes correlates with disease activity in patients with head and neck cancer. Clin Cancer Res 23: 4843-4854, 2017.
30. Troyer RM, Ruby CE, Goodall CP, Yang L, Maier CS, Albarqi HA, Brady JV, Bathke K, Taratula O, Mourich D and Bracha S: Exosomes from osteosarcoma and normal osteoblast differ in proteomic cargo and immunomodulatory effects on T cells. Exp Cell Res 358: 369-376, 2017.

31. Szczepanski MJ, Szajnik M, Welsh A, Whiteside TL and Boyiadzis M: Blast-derived microvesicles in sera from patients with acute myeloid leukemia suppress natural killer cell function via membrane-associated transforming growth factor-beta1. Haematologica 96: 1302-1309, 2011.
32. Kunigelis KE and Graner MW: The dichotomy of tumor exosomes (TEX) in cancer immunity: Is it all in the ConTEXt? Vaccines (Basel) 3: 1019-1051, 2015.
33. Mignot G, Roux S, Thery C, Ségura E and Zitvogel L: Prospects for exosomes in immunotherapy of cancer. J Cell Mol Med 10: 376-388, 2006.
34. Rao Q, Zuo B, Lu Z, Gao X, You A, Wu C, Du Z and Yin H: Tumor-derived exosomes elicit tumor suppression in murine hepatocellular carcinoma models and humans in vitro. Hepatology 64: 456-472, 2016.
35. Ichim TE, Zhong Z, Kaushal S, Zheng X, Ren X, Hao X, Joyce JA, Hanley HH, Riordan NH, Koropatnick J, *et al*: Exosomes as a tumor immune escape mechanism: Possible therapeutic implications. J Transl Med 6: 37, 2008.
36. Vignaux F, Vivier E, Malissen B, Depraetere V, Nagata S and Golstein P: TCR/CD3 coupling to Fas-based cytotoxicity. J Exp Med 181: 781-786, 1995.
37. Lenardo M, Chan KM, Hornung F, McFarland H, Siegel R, Wang J and Zheng L: Mature T lymphocyte apoptosis-immune regulation in a dynamic and unpredictable antigenic environment. Annu Rev Immunol 17: 221-253, 1999.
38. Kang YT, Kim YJ, Bu J, Cho YH, Han SW and Moon BI: High-purity capture and release of circulating exosomes using an exosome-specific dual-patterned immunofiltration (ExoDIF) device. Nanoscale 9: 13495-13505, 2017.
39. Dai S, Wei D, Wu Z, Zhou X, Wei X and Huang H: Phase I clinical trial of autologous ascites-derived exosomes combined with GM-CSF for colorectal cancer. Mol Ther 16: 782-790, 2008.